The Influence of State-of-Mix on the Extrudate Swell of a Carbon Black-Filled Styrene–Butadiene Rubber Compound

P. K. FREAKLEY, C. SIRISINHA

Rubber Process Engineering Centre, Institute of Polymer Technology and Materials Engineering, Loughborough University, Loughborough, Leicestershire, LE11 3TU, United Kingdom

Received 16 July 1996; accepted 10 December 1996

ABSTRACT: The factors which govern the extrudate swell of a styrene–butadiene rubber compound filled with 30 phr of N330 carbon black at various states-of-mix were investigated. The state-of-mix is quantified by an effective filler volume fraction, based on an estimate of the amount of rubber immobilized in the carbon black agglomerates. The swell has been found to be dominated by recoverable strain and relaxation time, which are both controlled by the effective filler volume fraction. In contrast, shear rate, wall slip, and the rubber–carbon black network have not been found to have a significant effect on the extrudate swell. © 1997 John Wiley & Sons, Inc. J Appl Polym Sci **65:** 305–315, 1997

Key words: extrudate swell; rubber; state-of-mix

INTRODUCTION

It is well known that extrudate swell is affected by the state-of-mix and that extrudate swell increases as filler dispersion improves.[1–3] In contrast, an increase in filler loading results in a decrease in the extrudate swell and is attributed to a reduction in the elastic phase of the rubber compound (dilution effect).[1,4–7] A reduction in the extrudate swell also occurs if the carbon black structure is increased or particle size decreased.[1,6] These observations can be unified by use of the concept of the effective filler volume fraction (EFVF) as a measure of the state-of-mix.[8]

During incorporation in the mixing process, rubber enters the internal voids of the carbon black agglomerates and becomes immobilized. As dispersive mixing progresses, the agglomerates are broken down into their component aggregates and the immobilized rubber is released. Thus, the EFVF rises to a maximum and then diminishes until, in the fully disagglomerated state, it is equal to the actual filler volume fraction. A change of the state-of-mix can therefore be considered to be equivalent to a change of filler loading and an increase in structure will provide more void volume for the immobilization of rubber.

Although the preceding observations suggest that the proposed dilution effect of filler loading on extrudate swell can also be applied to the effect of the state-of-mix, through the use of the EFVF, there are other factors related to the state-of-mix which need to be considered. These include wall slip, reformation of the tridimensional rubber–carbon network after emergence from the die, strain rate, and strain history. The magnitude of the effect which wall slip and strain history can exert will also be dependent on the die geometry. Normally, extrudate swell decreases with increasing die length until it levels off. The decrease is caused by relaxation of the elongational stresses generated at the die entrance. The leveling off of extrudate swell observed in long dies is controlled by the steady-state shear stress.[9–13] In addition, an increase in the contraction ratio has also been found to increase extrudate swell due to an increase in elongational stress.[14] An increase in

Correspondence to: P. K. Freakley.
 CCC 0021-8995/97/020305-11

shear stress and/or shear rate normally results in increasing the extrudate swell.[11,13] However, an insensitivity of the extrudate swell to the shear rate has been reported by other workers.[15,16] The objective of the work reported here was to identify the factors which exert a significant influence on the extrudate swell and to relate them quantitatively to the state-of-mix, as measured by the EFVF.

EXPERIMENTAL

Mixing

A simple rubber compound comprising styrene–butadiene rubber (SBR 1502) and 30 phr carbon black (N330) was used for all the experiments. The rubber compound was mixed in a Francis Shaw K1 Intermix with a fill factor of 0.5, a circulating water temperature of 30°C, and a rotor speed of 30 rpm. The SBR was first masticated for 90 s; thereafter, the carbon black was added and batches produced with incorporation and dispersion mixing times of 90, 120, 180, 300, and 600 s. The batches were then used as discharged, to avoid the additional mixing caused by sheeting off with a two-roll mill.

Investigation of Extrudate Swell

A Davenport capillary rheometer, with a barrel diameter of 20 mm and with a Dynisco pressure transducer sited just above the die, was used for all the extrusion rheometry measurements. Small pieces of compounded rubber were filled into the Davenport rheometer barrel and preheated at 120°C for 5 min. Three dies of 2 mm diameter with L/D ratios of 0 (approximately), 5, and 10 and conventional 90° entrance angles were used. Extrudate swell was determined at true wall shear rates of 21.38, 45.71, 97.72, 208.93, and 446.68 s^{-1}.

To measure the extrudate swell, the extrudates emerging from the dies were quenched immediately using cold water and their diameters were measured using a shadow microscope with a magnification power of 10×. Extrudate swell (B) is defined conventionally by the ratio of the extrudate diameter to the die diameter.

Investigation of Effective Filler Volume Fraction (EFVF)

The effective volume fraction of filler (ϕ_e) of can be quantified by[8]

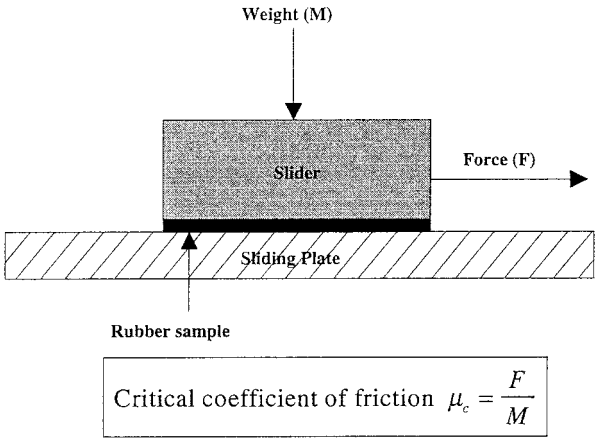

Figure 1 Friction slider.

$$\phi_e = (\alpha\phi_a) + \phi_t, \qquad (1)$$

where ϕ_e = effective volume fraction of filler, ϕ_a = volume fraction of agglomerates (equivalent to area fraction of agglomerates in thin section), ϕ_t = true volume fraction of carbon black (as calculated from the true density of carbon black, 1.8 g/cm^3), and α = volume fraction of occluded rubber in an agglomerate (0.647 for N330, from the DBP absorption value quoted by Cabot). The area fraction of remaining agglomerates at each mixing time was determined by light microscopy at a magnification of 250× and the use of a simple PC-based computer-aided image analysis package (VIDS, AI Ltd, Cambridge, UK). Agglomerates ≥ 4 μm were detected by this method.

Investigation of Wall Slip with Rotational Rheometry

A Negretti TMS biconical rotor rheometer was used to determine the amount of wall slip. The rubber sample to be tested was preheated at 120°C for 5 min. Thereafter, shear stresses were measured at sequential shear rates of 10, 20, 40, and 80 s^{-1} using grooved and smooth rotors. The shear stresses from smooth and grooved rotors were compared for differences which would indicate slippage on the smooth rotor.

Prediction of the Onset of Wall Slip in the Die from Friction Measurements

Values of the critical coefficient of friction (μ_c) for the onset of slippage were obtained using the slider method with different loading weights at the test temperature of 120°C. A schematic of the apparatus used is shown in Figure 1. Shear stress

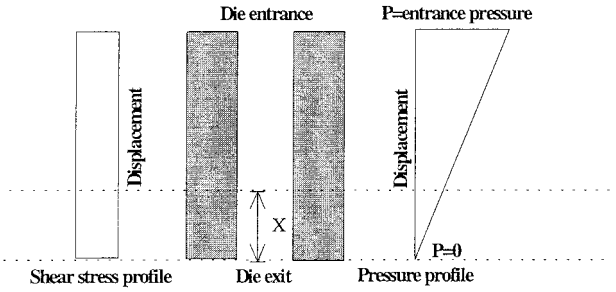

Figure 2 Schematic model of the pressure profile used for the calculation of the onset of wall slip.

is obtained from the capillary results. Therefore, pressure at the onset of slip can be obtained from eq. (2). Thereafter, by substituting the calculated pressure at the onset of slip in eq. (3), the displacement from the die exit at the onset of wall slip (distance X in the Fig. 2) can be obtained. It is assumed that that the pressure decreases linearly with displacement from the die entrance to zero at the die exit and that shear stress at the die wall is constant along the die land, as shown in Figure 2:

$$P = \frac{\tau_w}{\mu_c} \tag{2}$$

$$P_{(X)} = AX + B \tag{3}$$

where τ_w = shear stress at wall which is a function of shear rate and μ_c = critical frictional coefficient (equal to 1.35 for all the mixing times investigated).

Investigation of Rubber–Carbon Black Tridimensional Transient Network

The Monsanto (Flexsys) rubber processability analyzer (RPA2000) was utilized for quantifying the rubber–carbon black network. After a preheat time of 120 s, sequential strain amplitudes of 1, 560, and 1% were applied to the rubber compounds at the test temperature of 120°C and frequencies of 0.5, 10, and 10 Hz, respectively. Storage shear modulus, loss modulus, and tan δ were calculated using the RPA software[17,18] and plotted as a function of time. From the form of the storage shear modulus vs. time plot at 1% strain amplitude after conditioning at the 560% amplitude and comparison with the initial 1% strain amplitude result, it is possible to determine if there is a rubber–carbon black network and, if so, to assess the extent of breakdown and the rate of reformation.

Estimation of Relaxation Time

Storage shear modulus (G') was measured using the Monsanto RPA at a frequency of 0.5 Hz and strain amplitude of 1%. Shear viscosity was obtained from capillary results. From the Cox and Merz concept,[19] a frequency of 1 rad per s is equivalent to the shear rate of 1 reciprocal second. Consequently, the shear viscosity at a shear rate of 3.14 s^{-1} and storage modulus at a frequency of 0.5 Hz, at a test temperature of 120°C, were used to calculate the relaxation time:

$$\Gamma = \frac{\eta_{3.14}}{G'_{3.14}} \tag{4}$$

where $\eta_{3.14}$ = shear viscosity at shear rate of 3.14 s^{-1} and $G'_{3.14}$ = storage shear modulus at % strain of 1 and frequency of 0.5 Hz.

RESULTS AND DISCUSSION

Relationship Between State-of-Mix and Extrudate Swell

As expected, it can be seen from Figure 3 that the effective volume fraction of the filler (EFVF) decreases with an increase in mixing time, which can be explained by the release of immobilized rubber.[8] The EFVF for the compound mixed for 600 s approaches the value of the true volume fraction of N330 carbon black, indicating that most of the carbon black is in separated aggregates.

It can be seen from Figure 4 that extrudate swell increases with increasing mixing times, as reported by Pliskin[1] and Figure 5 shows that this effect can be attributed to the change in the state-of-mix. At this point, it is not possible to conclude that there is a direct relationship between extrudate swell and EFVF without additional evidence to eliminate other factors which may also be dependent on the state-of-mix and influential on the extrudate swell.

Consideration of the Influence of Wall Slip on Extrudate Swell

Since it is known that, at constant volumetric flow, shear stress decreases with an increase in

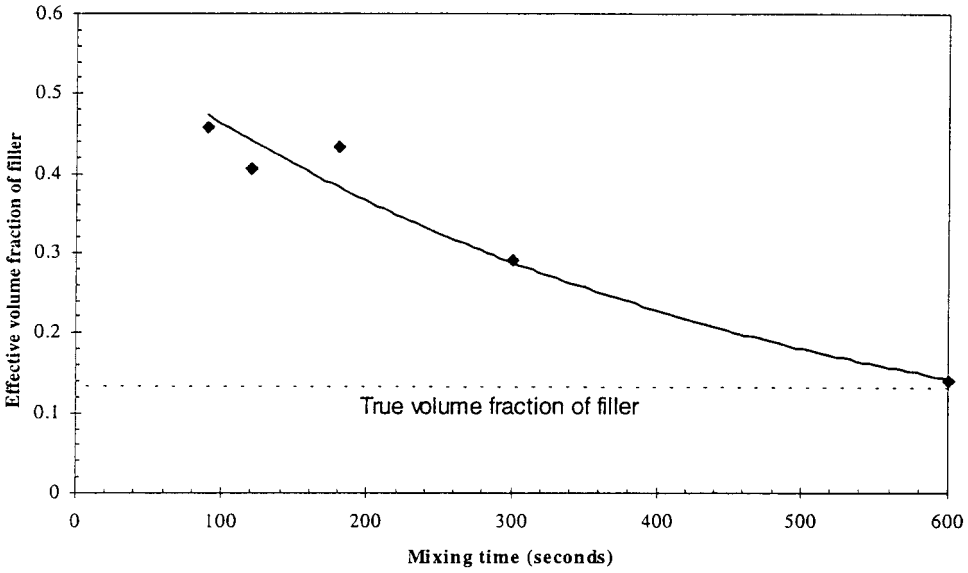

Figure 3 Relationship between mixing time and experimental effective volume fraction of filler (EFVF).

wall slip, extrudate swell will also reduce with increasing wall slip. The classical Mooney technique is not valid for the present study because it is based on the assumption that wall shear stress, slip velocity, and pressure gradient are constant along the length of the die land and independent of the die diameter.[12,20,21] Therefore, two other methods were used: direct measurement with the Negretti TMS biconical rotor rheometer and calculation of the onset of wall slip in the die from friction slider tests.

Evidence of wall slip was obtained from a Negretti TMS biconical rotor rheometer by comparison of the shear stresses from grooved and smooth rotors at a specified shear rates. The badly mixed compound (mixing time of 90 s) was selected for this test because experience has shown that wall slip diminishes as the state-of-mix improves. The result in Figure 6 shows little difference in shear stress measured from smooth and grooved rotors for the whole range of shear rates. Despite this result, the possibility that wall slip influences extrudate swell cannot yet be eliminated. Near the exit of the capillary die, high shear stresses, which are dependent on the state-of-mix, occur in conduction with low pressure, as shown by Figure 2. This is the region where flow velocity equalization occurs and is the origin of the die exit effect.

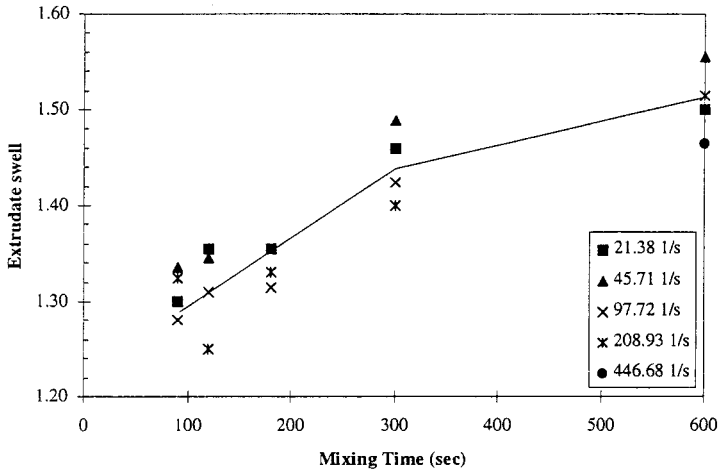

Figure 4 Relationship between extrudate swell and mixing time ($L/D = 5$).

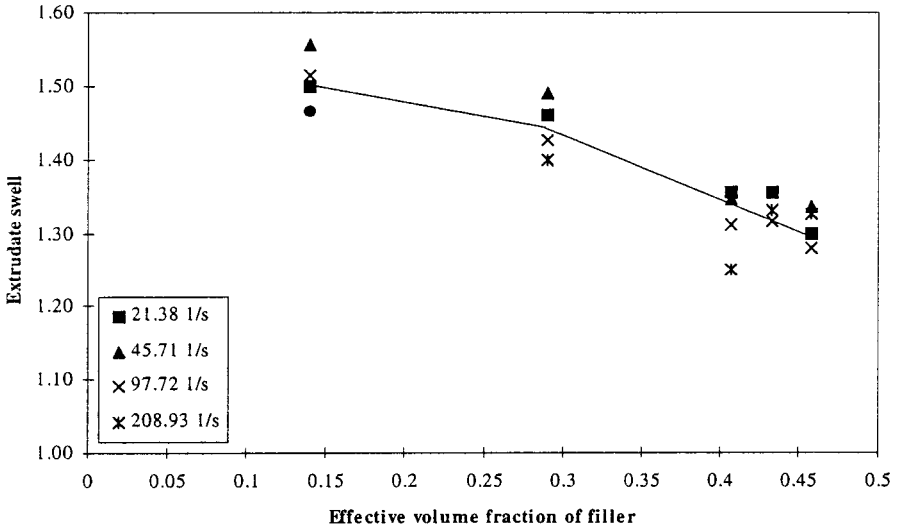

Figure 5 Effect of effective volume fraction of filler on extrudate well ($L/D = 5$).

The critical coefficient of friction for the initiation of slip was determined by a friction slider and found to be independent of the state-of-mix, with a value of 1.35. As Figure 7 shows, the badly mixed compounds start to slip slightly further from the die exit than do the well mixed ones due to differences in flow behavior but the effect is insignificant and wall slip can now be eliminated as a source of the dependence of the extrudate swell on the state-of-mix.

Consideration of the Influence of the Rubber–Carbon Black Network on Extrudate Swell

The level of carbon black in the compound used for this study, at 30 phr, is below the loading at which formation of a rubber–carbon black network is considered to be possible.[22] However, as Figure 3 shows, immobilized rubber causes the effective filler loading in the compounds with short mixing times to be over 100 phr, so this effect must be considered. The rubber–carbon black network will suppress extrudate swell if it can reform rapidly in the deformed state (region X in Fig. 8) because the coiling up force of the oriented molecules will be opposed by the network. Therefore, one can expect that this network should result in a decrease in relaxation time and recoverable shear and thus a reduction in extrudate swell.

The Monsanto RPA2000 instrument was used

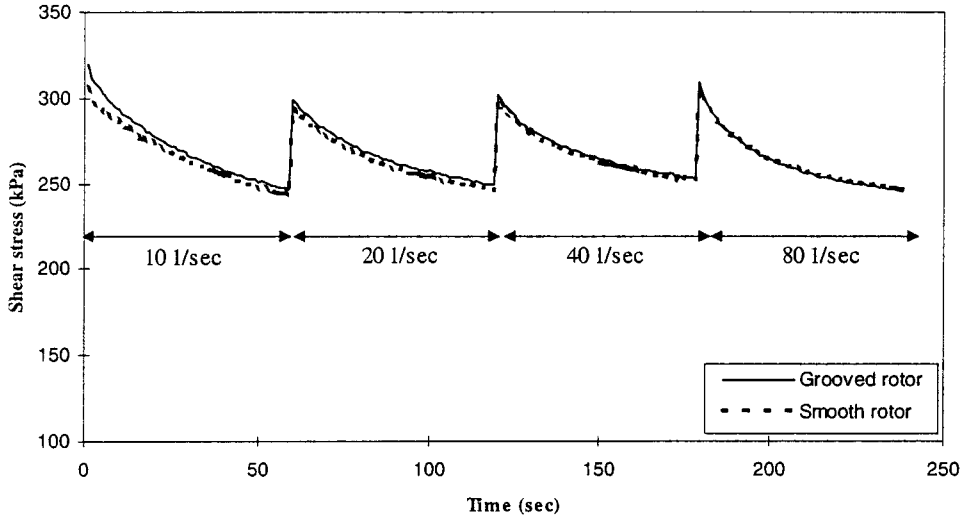

Figure 6 Investigation of wall slip in the die of a badly mixed compound (mixing time of 90 s) using the Negretti TMS biconical rotor rheometer (varying shear rate).

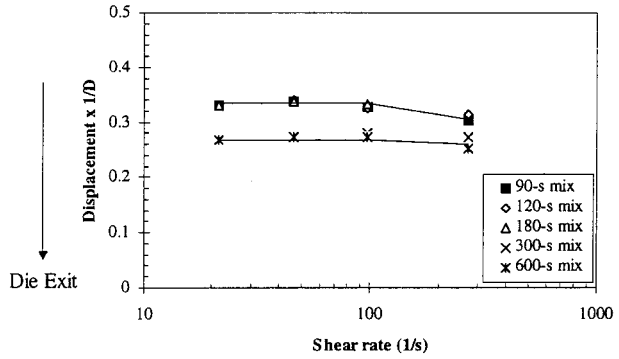

Figure 7 Displacement in the die land at the onset of wall slip ($L/D = 5$).

for analyzing the rubber–carbon black tridimensional transient network. Initially, the storage shear modulus was measured at a low strain amplitude of 1% to minimize disruption of any rubber–carbon black network formed during the preheat period. Subsequently, a strain amplitude of 560% was applied to disrupt the network and the sample was then sheared again at a low strain amplitude of 1% to allow the network to reform. Comparison of the results in Figure 9 with those of other workers[22] shows that a rubber compound with 30 phr of carbon black does not demonstrate significant network effects, even though the EFVF is high in the sample tested. Presumably, this can be attributed to most of the carbon black being in the form of agglomerates with a low effective specific surface area and comparatively large interagglomerate spacings.

As a further verification of the absence of a rubber–carbon black network, it can be seen from Figure 10 that the values of relative modulus (G'_{cpd}/G'_{gum}) obtained from the Monsanto RPA2000 are in good agreement with the Guth and Gold equation:

$$\frac{G'_{cpd}}{G'_{gum}} = 1 + 2.5 \cdot \phi_e + 14.1 \cdot \phi_e^2 \qquad (5)$$

where G'_{cpd} and G'_{gum} = the storage modulus mea-

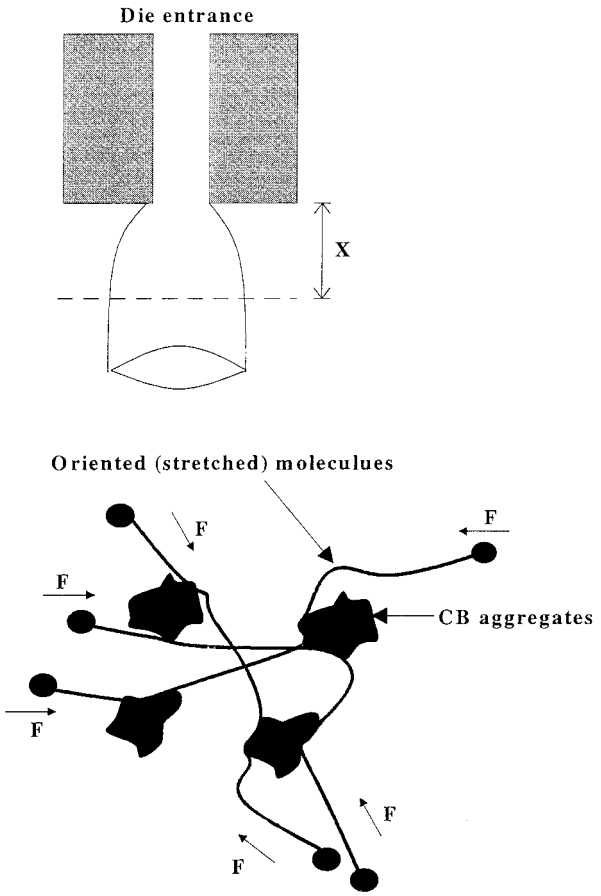

Figure 8 Rubber–carbon black tridimensional transient network in a deformed state (extended state) where the network reforms.

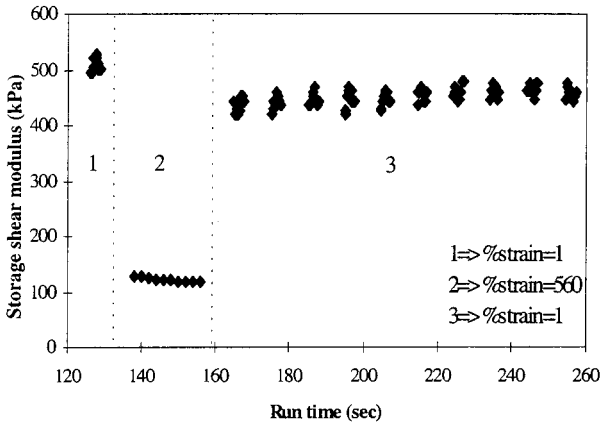

Figure 9 An absence of carbon black–rubber tridimensional transient network (mixing time of 90 s).

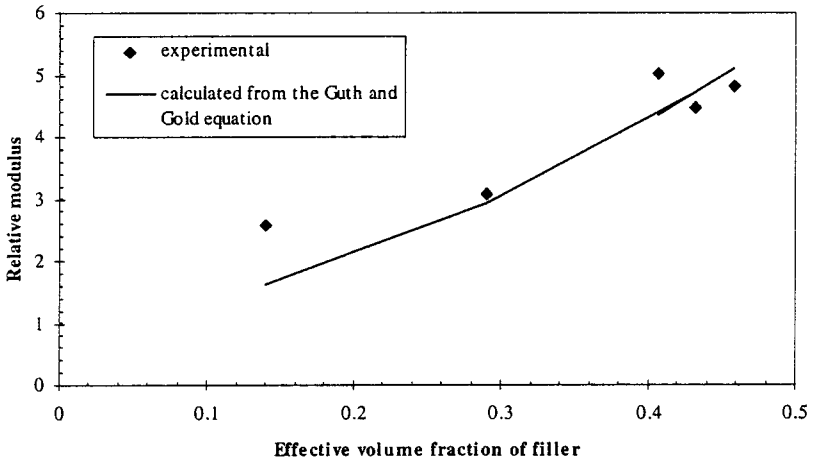

Figure 10 Relationship between the relative modulus obtained from the Monsanto RPA2000 result and calculation based on the Guth and Gold equation.

sured from the RPA2000 for the compounds and gum, respectively, and ϕ_e = the effective volume fraction of filler.

Consideration of the Influence of Effective Filler Volume Fraction on Extrudate Swell

Now that the state-of-mix dependence of wall slip and the rubber–carbon black network have been eliminated as contributors to extrudate swell, it is possible to assign the effect directly to the EFVF and to consider the mode of action in detail. Referring again to Figure 5, it can be seen that extrudate swell increases substantially with decreasing EFVF. For a badly mixed compound, the high EFVF indicates a great amount of immobilized rubber and only a small amount of free rubber with elastic memory. In contrast, for the well-mixed compound with a low EFVF, the amount of free rubber is large, which results in the high elastic response (high extrudate swell). Similar trends have been reported previously.[1]

From Fig. 11, it can be seen that extrudate swell is related strongly to shear modulus. Although it is tempting to conclude simply that a low shear modulus will result in a greater recoverable strain and extrudate swell,[23] it has to be borne in mind that the Guth–Gold equation predicts that changing the EFVF will have a similar effect on both on the modulus and viscosity; therefore, a high modulus will be associated with high stress in the capillary. However, rubber compounds are strongly non-Newtonian in their flow behavior and the relationships of shear modulus and shear stress at the capillary wall with EFVF may be dissimilar. The proposal can be verified

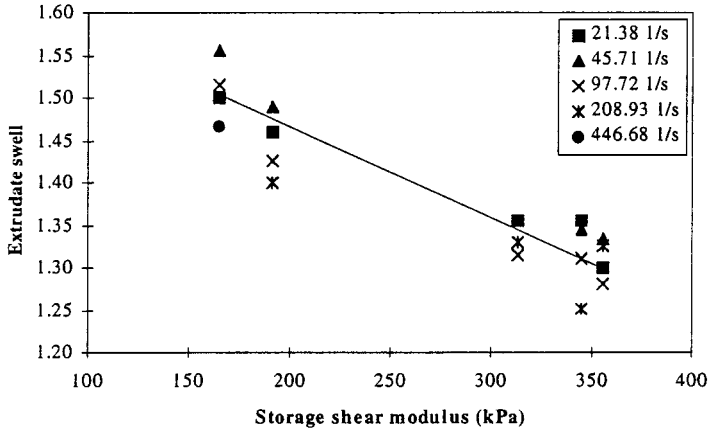

Figure 11 Relationship between extrudate (L/D = 5) and storage shear modulus at 0.5% shear strain.

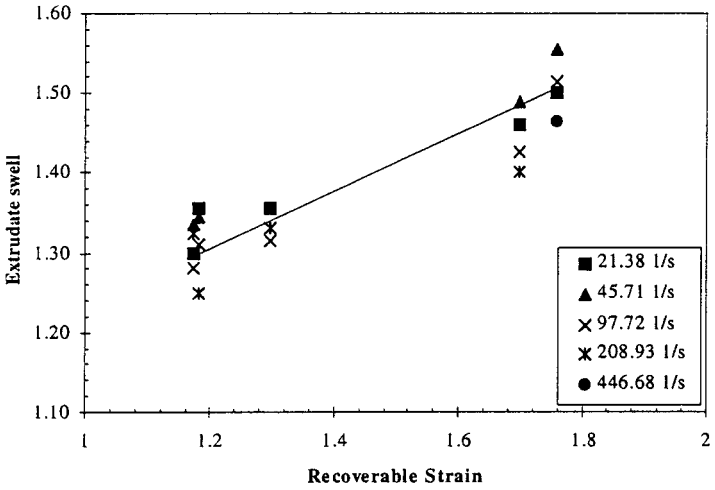

Figure 12 Relationship between extrudate swell (L/D = 5) and recoverable shear strain (under % strain of 0.5, shear stress at shear rate of 21.38 s^{-1}).

by calculation of recoverable shear from the shear stress at the capillary wall and the storage shear modulus from the Monsanto RPA2000:

$$\gamma_R = \frac{\tau_{true}}{G'} \tag{6}$$

where γ_R = recoverable shear strain, τ_{true} = true shear stress at wall, and G' = storage shear modulus.

Figure 12 confirms that the relationships of wall shear stress and shear modulus with EFVF are dissimilar and that extrudate swell and recoverable strain are strongly related. However, in dies of low L/D ratio, entrance effects persist to exert a strong influence on extrudate swell and the recoverable strain concept, which is associated with flow in the steady-state flow region of a capillary, may not be applicable. Figure 13 shows that up to an L/D ratio of 5 extrudate swell is influenced strongly by the memory of the elongational flows in the die entrance. The decay of the

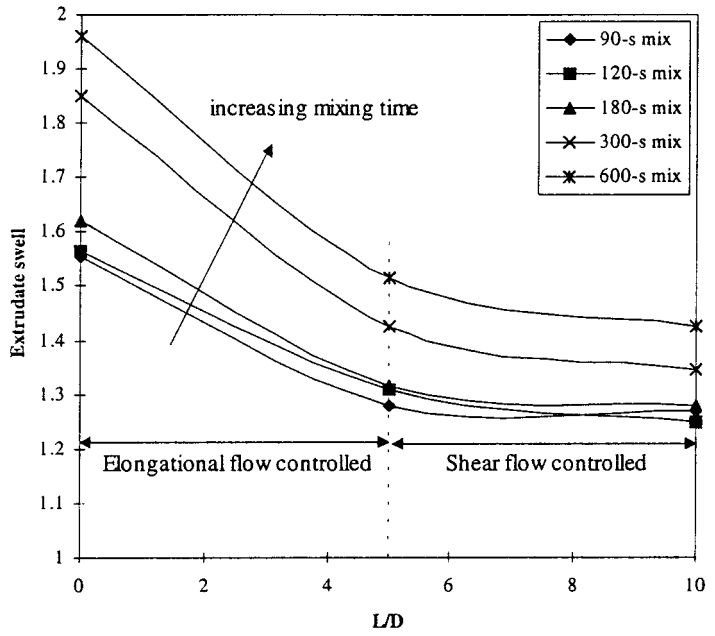

Figure 13 Effect of die length on extrudate swell of the SBR compounds at shear rate of 97.72 s^{-1}.

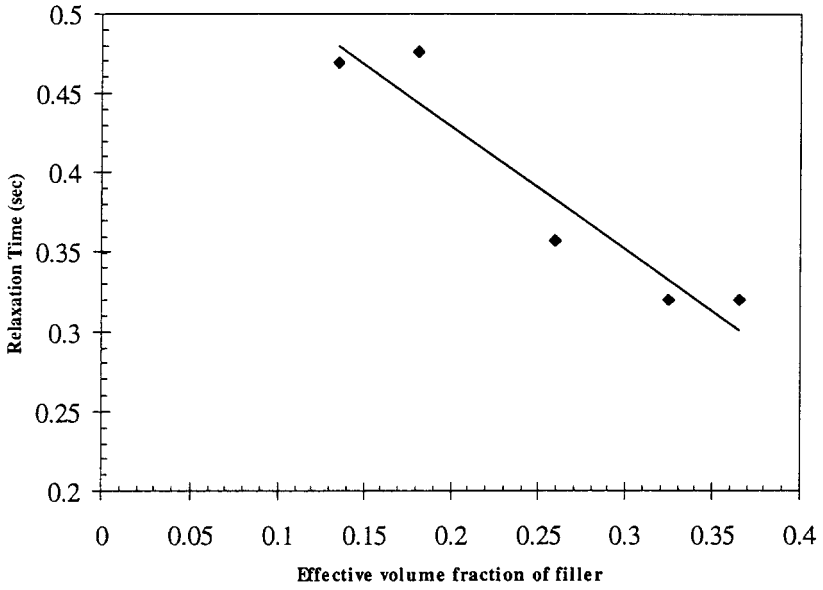

Figure 14 Relationship between relaxation time and effective volume fraction of filler ($L/D = 5$).

viscoelastic memory is a relaxation process, so it is useful to examine the relationship of EFVF and relaxation time, defined as the ratio of shear viscosity to shear modulus. Although the relaxation processes in the capillary are elongational rather than shear, Figure 14 indicates that the memory of entrance effects is more persistent in well-mixed compounds and, as expected, Figure 15 shows that extrudate swell and relaxation time are related. In addition, Figure 16 shows a proportionality between relaxation time and recoverable shear, which suggests that they share a similar dependence on EFVF. Thus, the form of the relationship between extrudate swell and EFVF can be expected to be maintained irrespective of die geometry.

Consideration of the Influence of Shear Rate on Extrudate Swell

Figure 17 clearly indicates an insensitivity of extrudate swell to shear rate. Although an increase in shear rate tends to increase extrudate swell, due to an increase in shear stress and a reduction of residence time, the associated rise in melt temperature caused by viscous dissipation contri-

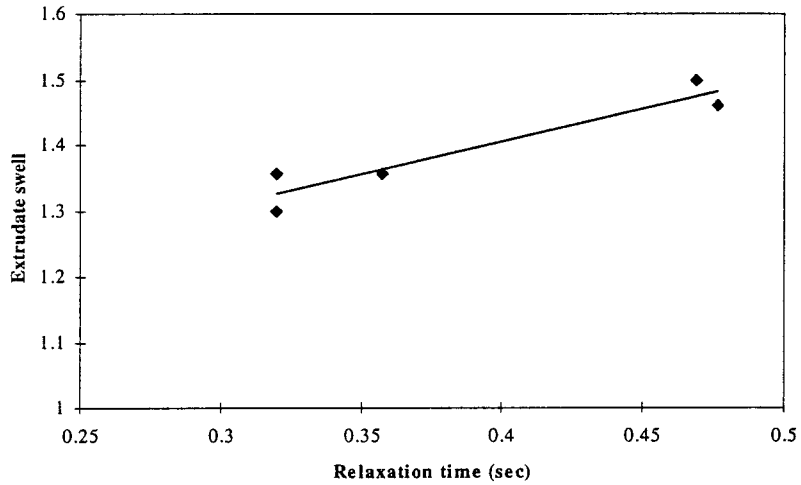

Figure 15 Relationship between relaxation time and extrudate swell ($L/D = 5$).

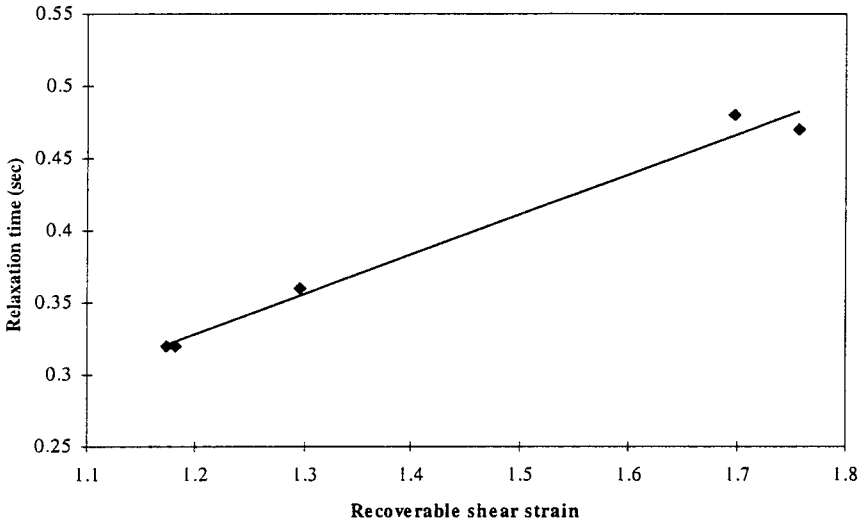

Figure 16 Relationship between relaxation time and recoverable shear strain (under % strain of 0.5, shear stress at shear rate of 21.38 s^{-1}; $L/D = 5$).

butes to a decrease in the extrudate swell. If these effects are equal in magnitude, the shear-rate insensitivity of the extrudate observed here and by other workers[15,16] will prevail. However, this hypothesis can only be confirmed by rigorous mathematical modeling of the viscoelastic processes in capillary flow.

CONCLUSIONS

1. Extrudate swell of the SBR + 30 phr N330 carbon black compound investigated is influenced strongly by the state-of-mix as quantified by the effective filler volume fraction (EFVF).
2. The SBR compound does not exhibit any rubber–carbon black network effects, even at high EFVF levels produced by short mixing times, and this effect could thus be eliminated as a potential influence on extrudate swell. The absence of a network was confirmed by the good agreement of the Guth–Gold equation with the dependence of relative modulus, determined from cyclic dynamic tests, on EFVF.
3. The critical coefficient of friction for wall slip was found to be independent of the state-of-mix and was eliminated as a po-

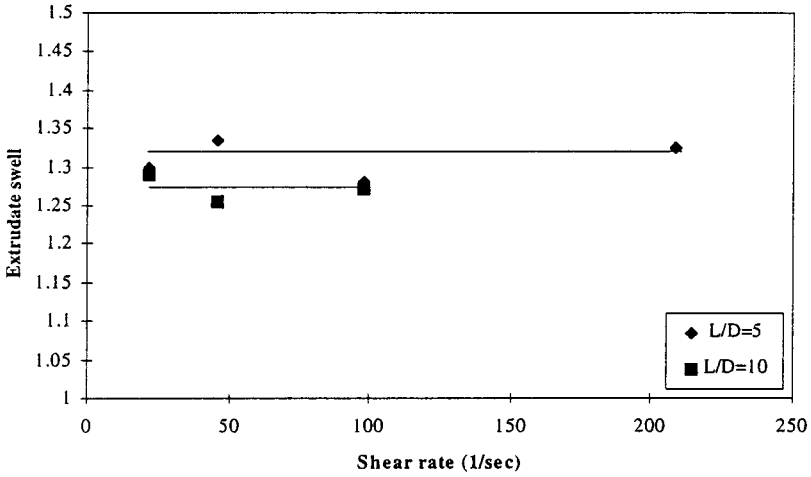

Figure 17 Effect of shear rate on extrudate swell (mixing time of 90 s).

tential mechanism for observed changes in extrudate swell with mixing time.
4. Both recoverable shear and relaxation time are similarly related to extrudate swell, have a linear proportionality with each other, and are controlled by EFVF. Thus, the form of the relationship of extrudate swell with EFVF will not be influenced by die geometry.
5. Shear modulus, determined from a cyclic dynamic test, shows a good relationship with extrudate swell and can be used a simple predictor of extrudate swell.

REFERENCES

1. I. Pliskin, *Rubb. Chem. Technol.,* **46,** 1218 (1973).
2. N. Tokita and I. Pliskin, *Rubb. Chem. Technol.,* **46,** 1116 (1973).
3. T. Nishimura and T. Kataoka, *Rheol. Acta,* **23,** 401 (1984).
4. E. A. Collins and J. T. Oetzel, *Rubb. Age,* **102,** 64 (1970).
5. J. M. Dealy and K. F. Wissbrun, *Melt Rheology and Its Role in Plastic Processing: Theory and Applications,* Van Nostrand Reinhold, New York, 1990.
6. K. C. Shin, J. L. White, and N. Nakajima, *J. Non-Newt. Fluid Mech.,* **37,** 95 (1990).
7. J. L. Leblanc, *Prog. Rubb. Plast. Technol.,* **10,** 112 (1994).
8. J. Clarke and P. K. Freakley, *Rubb. Chem. Technol.,* **67,** 945 (1994).
9. T. Ariai and H. Aoyama, *Trans. Soc. Rheol.,* **7,** 333 (1963).
10. E. B. Bagley, S. H. Storey, and D. C. West, *J. Appl. Polym. Sci.,* **7,** 1661 (1963).
11. J. S. Anand and I. S. Bhardwaj, *Rheol. Acta,* **19,** 614 (1980).
12. J. L. Leblanc, *Prog. Rubb. Plast. Technol.,* **5,** 173 (1989).
13. D. C. Huang and J. L. White, *Polym. Eng. Sci.,* **19,** 609 (1979).
14. C. D. Han and K. U. Kim, *Polym. Eng. Sci.,* **11,** 395 (1970).
15. N. Nakajima and D. A. Collins, *Rubb. Chem. Technol.,* **48,** 615 (1975).
16. V. M. Murty, B. R. Gupta, and S. K. De, *Plast. Rubb. Proc. Appl.,* **5,** 307 (1985).
17. A. Y. Coran and J. B. Donnet, *Rubb. Chem. Technol.,* **65,** 1016 (1992).
18. J. L. Leblanc, *Plast. Rubb. Comp. Proc. Appl.,* **24,** 241 (1995).
19. W. P. Cox and E. H. Merz, *J. Polym. Sci.,* **28,** 619 (1958).
20. S. G. Hatzikiriakos and J. M. Dealy, *J. Rheol.,* **36,** 845 (1992).
21. P. Mourniac, J. F. Agassant, and B. Vergnes, *Rheol. Acta,* **31,** 65 (1992).
22. J. S. Dick and H. A. Pawloski, Paper presented at a Meeting of the Rubber Division, American Chemical Society, Denver, Colorado, May 18–21, 1993.
23. F. N. Cogswell, *Polym. Eng. Sci.,* **12,** 64 (1972).